TABLES

Path	Row(s)	Date	Use
39	32-34	6 May 2004	N-E
39	32-34	7 June 2004	N-L
39	34	20 April 2004	N-E
39	34	6 March 2005	S-E
39	34	25 May 2005	S-L
39	34	26 June 2005	S-L
39	34	7 April 2005	S-L
39	35-36	2 February 2005	S-E
39	35-36	23 April 2005	S-L
39	35-36	9 May 2005	S-L
40	31-32	30 June 2004	N-L
40	31-33	11 April 2004	N-E
40	31-33	27 April 2004	N-E
40	32-33	14 June 2004	N-L
40	34	13 March 2005	S-E
40	34-35	29 March 2005	S-E
40	34-35	14 April 2005	S-L
41	31-33	4 May 2004	N-E
41	31-33	21 June 2004	N-L
41	34	21 April 2005	S-L
41	34	23 May 2005	S-L
42	31-32	28 June 2004	N-L
42	31-33	25 April 2004	N-E
42	31-33	12 June 2004	N-L
42	34	12 April 2005	S-L
42	34	14 May 2005	S-L
42	34	30 May 2005	S-L
42	34	15 June 2005	S-L
43	31	5 July 2004	N-L
43	31-33	2 May 2004	N-E
43	31-33	19 June 2004	N-L

Table 1: Landsat 5 data purchase. *Use* indicates if a scene was used for the northern (N) or southern (S) set, and early (E) or late (L) season.

Variable Name	Description
Slope	Angle of topographic divergence from horizontal in degrees, default calculation in ENVI 4.2
Aspect	Angle of slope's face from true north in degrees, default calculation in ENVI 4.2
Heat Index	Mathematical combination of slope and aspect that correlates with the heat load of a topographic point ranging from 0 for 45 degree slopes with a northeast face to 1 for 45 degree slopes with a southwest face. Calculated in ENVI 4.2 using the function in Peterson (2000)
Exposure	Convexity of topography as measured by a pixel being higher than the average of surrounding pixels, from variable neighborhoods, combined with weighted averaging: $E = \frac{(P_i - N_3) * 4 + (P_i - N_9) * 3 + (P_i - N_{27}) * 2 + (P_i - N_{81})}{4 + 3 + 2 + 1}$ Where P_i is the value of the focal pixel and N_X is the average over a neighborhood of x by x pixels.
Aridity	Combines Heat Index and Exposure to provide maximum values for southwest facing convex features and minimal values for northeast facing concave features: [function]

Table 2: Geographic variables (GIS layers) derived from digital elevation model (DEM).

Dataset	Variable	Condition
LL04	raw data band 1, early season	≤ 65
	raw data band 1, early season	≥ 170
	NDVI, early season	< -0.12
	NDVI, late season	< -0.12
	NDVI, late season	> 0.28
LL05	raw data band 1, late season	>= 155

Table 3: Filters used to zero map pixels. These generally eliminate error in playas, forests, wetlands, and lakes where a false positive may occur due to phenology patterns or water reflection. Condition provides the mathematical statement that, when TRUE, results in a zeroing of the pixel value for annual grass cover.

Data Set	Variable	Coefficient	p-value
LL04 (*n*=689)	Intercept	-612.9975	0.0203
	NDVIearly	362.2552	0.000000293
	ΔNDVI + 2	414.7017	0.0177
	(ΔNDVI + 2)4	-11.3159	0.0362
	ELEV	-0.0222	0.000000187
	Region2	-20.3103	0.00143
	Region3	1.5568	0.483
	Region4&5	-4.4817	0.0549
	Region6	-10.5149	0.0107
	NDVIearly*ELEV	-0.1603	0.0000831
LL05 (*n*=130)	Intercept	58.4205	0.00000000000787
	NDVIearly	79.7398	0.000230
	ΔNDVI	-69.0320	0.00165
	ELEV	-0.0163	0.000115
	LateSeasonDate	-0.2737	0.00156
	DaysApart	0.0532	0.390
	Region3&7	12.8757	0.00397
	Region6	4.4046	0.335
MM04 (n=688)	Intercept	-524.1190	0.107
	NDVIearly	545.6410	0.000000000782
	ΔNDVI + 2	372.9796	0.0853
	(ΔNDVI + 2)4	-12.0503	0.0764
	ELEV	-0.0193	0.000160
	Region3	3.3588	0.137
	Region4&5	-5.3061	0.0209
	NDVIearly*ELEV	-0.2488	0.00000261
MM05 (*n*=118)	Intercept	22.1276	0.182
	NDVIearly	76.2708	0.138
	ΔNDVI	1.4205	0.988
	ELEV	-0.0230	0.0000000834
	Region6	5.0345	0.409

Table 4: Final models for each dataset. Ecoregion was included as a set of binary variables.

FIGURES

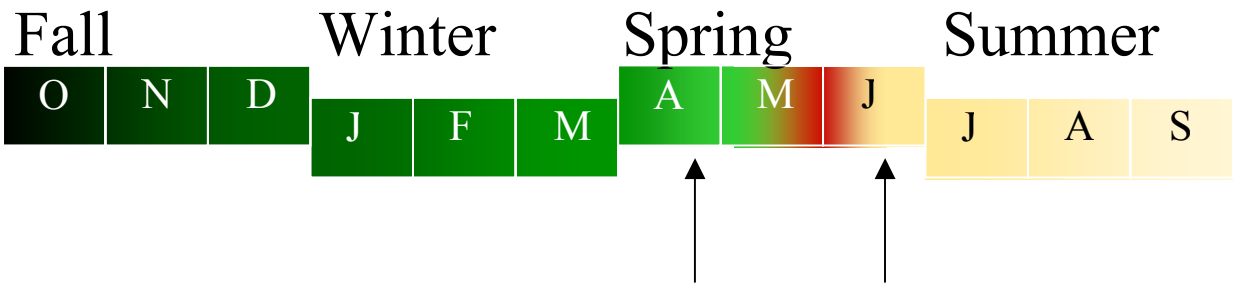

Figure 1: Illustration of phenology pattern for *Bromus tectorum*. Letters refer to months of the year. *B. tectorum* germinates after fall rains, over winters, then is ready for rapid growth in the spring. By late-May, it usually begins to senesce, first turning purplish-red, then drying out to straw-yellow. Arrows indicate optimal timing for satellite sensor data (imagery) with the first data collection during optimal growth and the second data collection just after yellowing, while most other vegetation remains active.

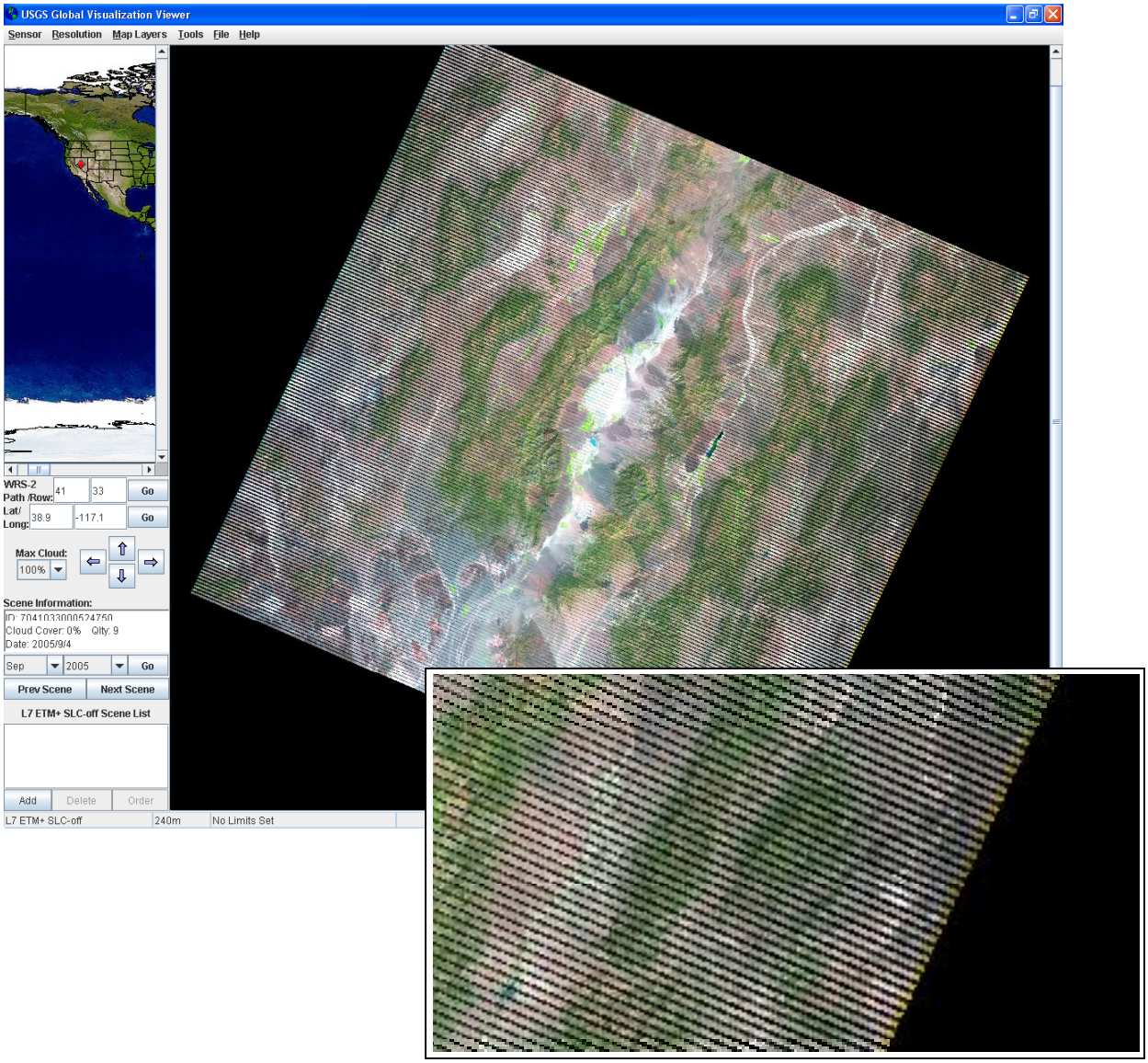

Figure 2: Landsat 7 SLC-off imagery preview from U.S.G.S. Global Visualization Viewer (U.S.G.S. 2006), magnified in inset.

Early 2004

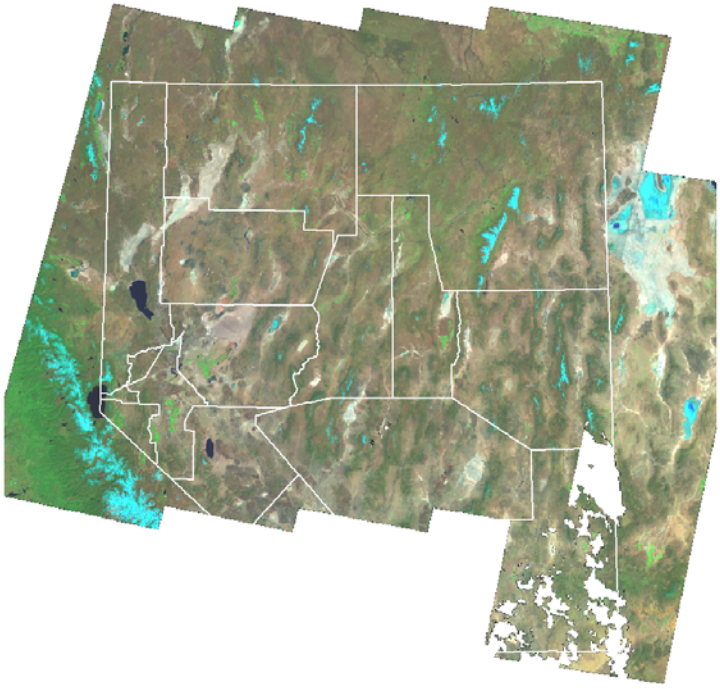

Late 2004

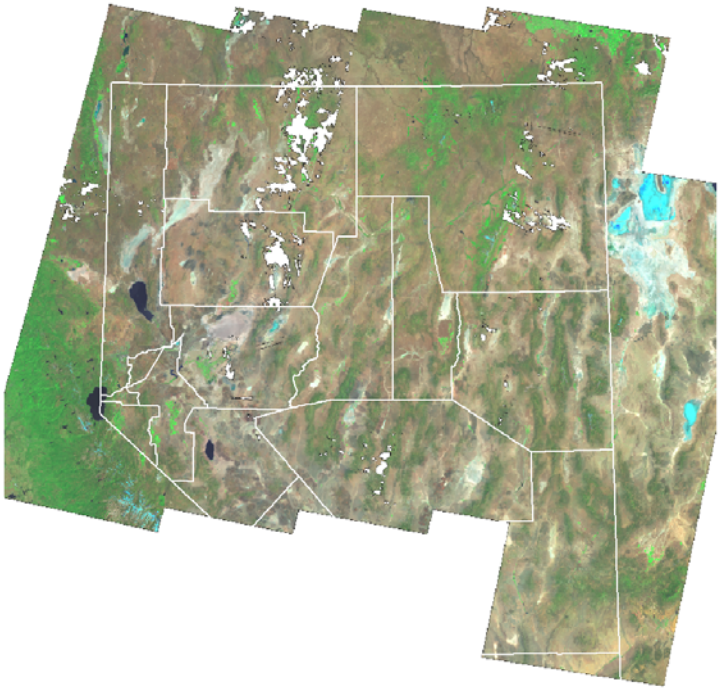

Figure 3: Early and late season satellite sensor data sets, viewed as false color images, for the northern portion of the state, collected in 2004. County boundaries are overlaid in white. False color is rendered with Landsat 5 bands 7, 4, and 2 for red, green, and blue channels, respectively.

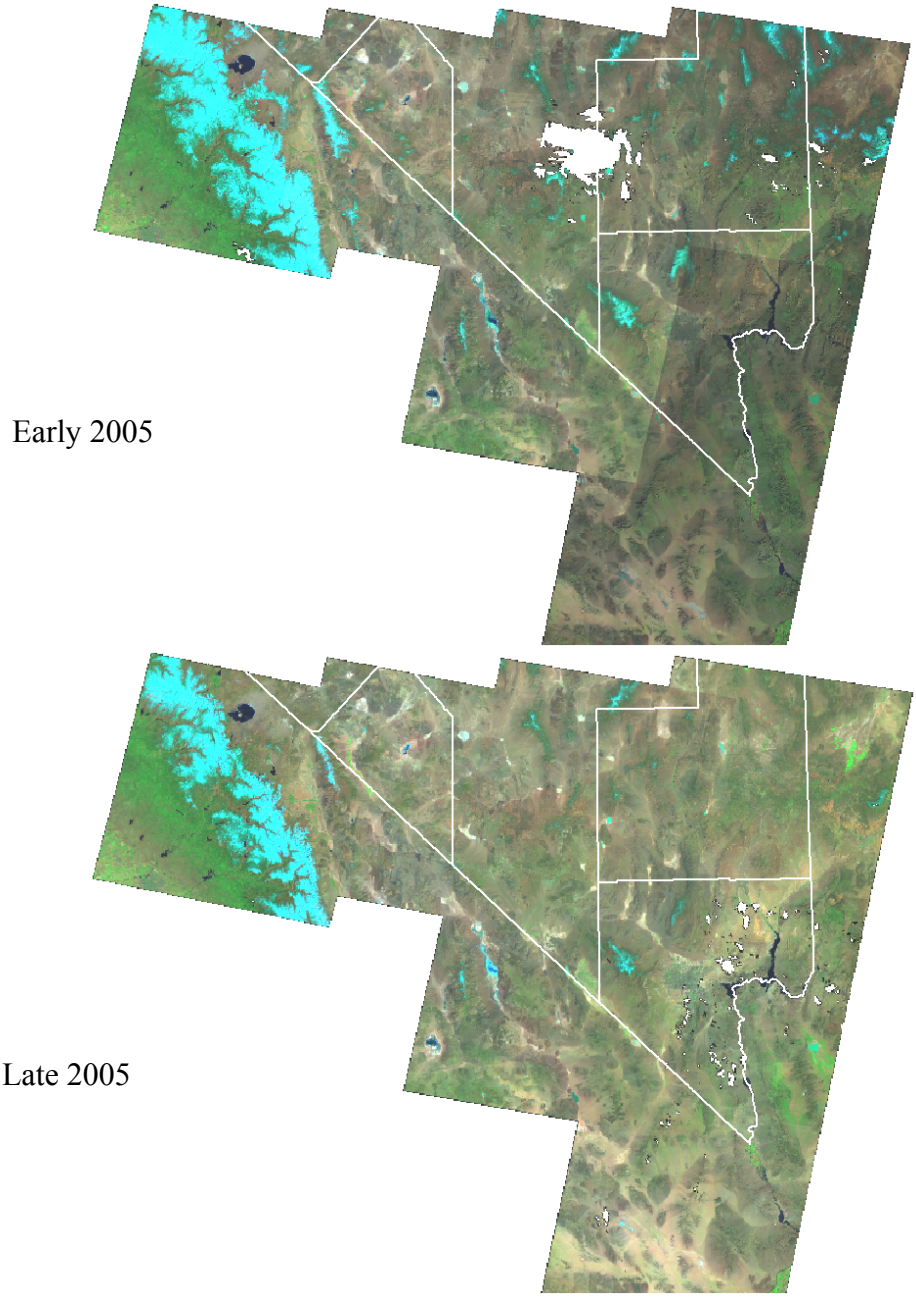

Figure 4: Early and late season satellite sensor data sets, viewed as false color images, for the southern portion of the state, collected in 2005. County boundaries are overlaid in white. False color is rendered with Landsat 5 bands 7, 4, and 2 for red, green, and blue channels, respectively.

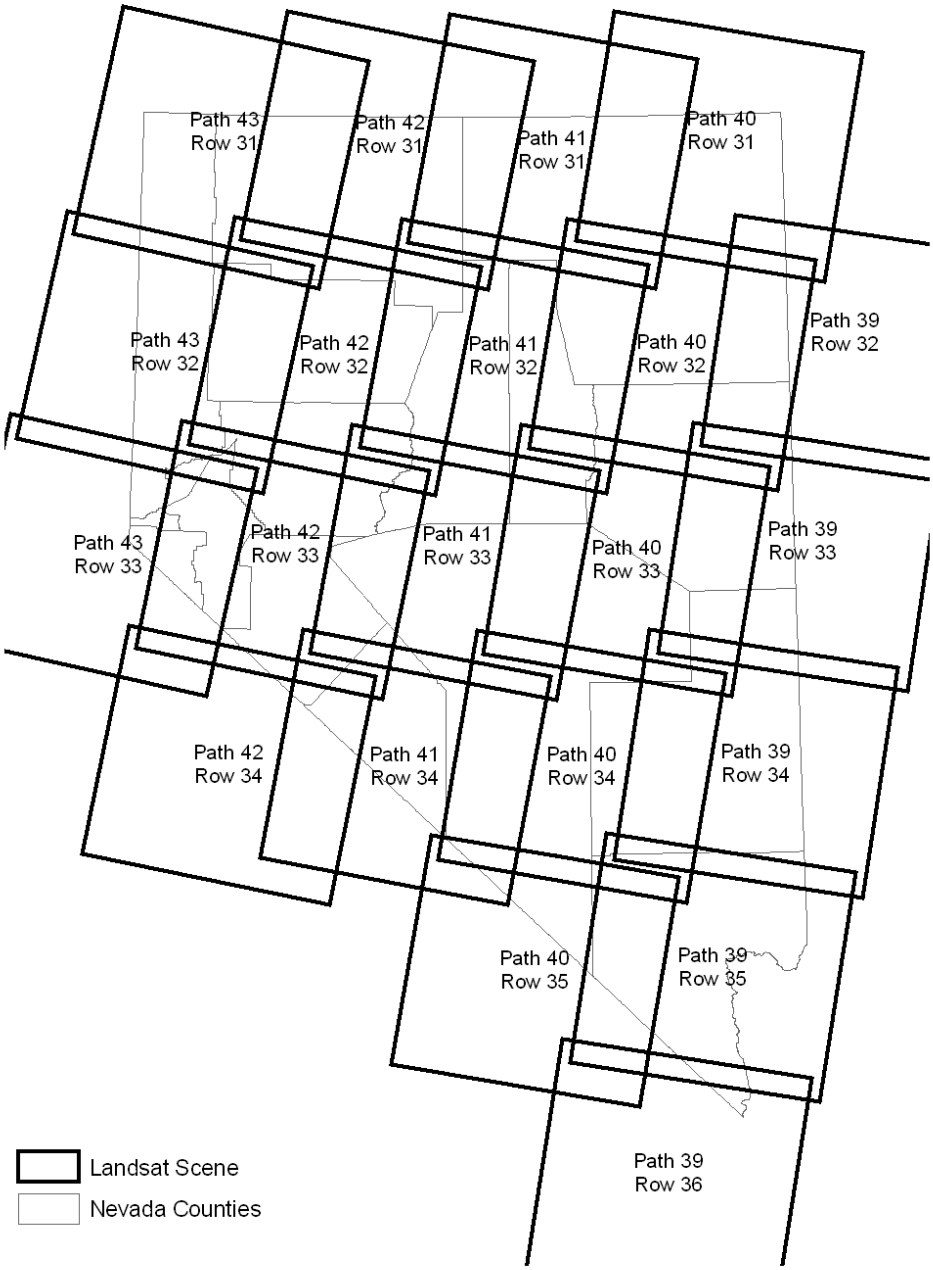

Figure 5: Landsat series satellite scene coverage for the state of Nevada.

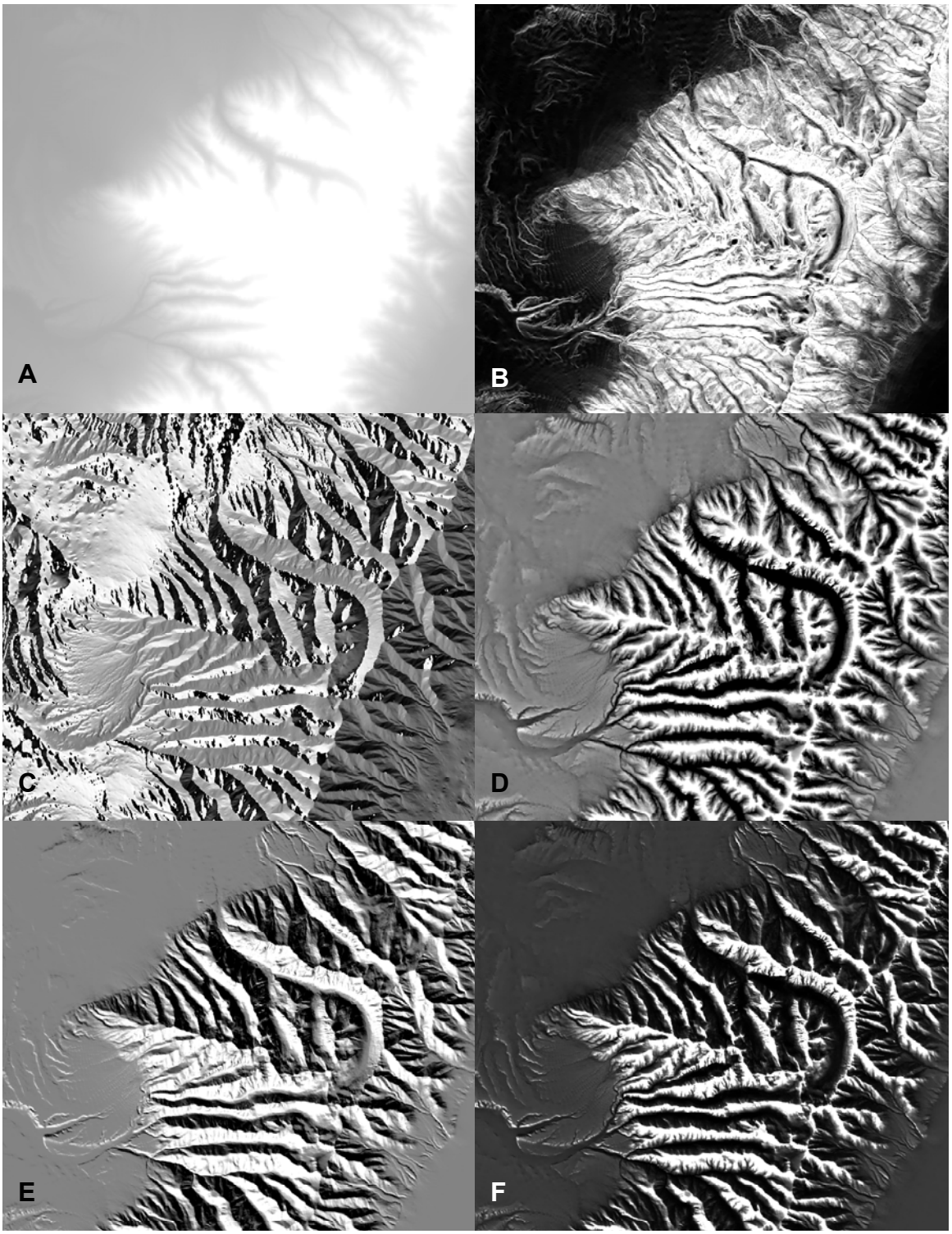

Figure 6: Digital elevation model and derived variables demonstrated with a view of the Ruby Mountains, including Lamoille Canyon, Elko County. **A:** Elevation. **B:** Slope. **C:** Aspect. **D:** Exposure. **E:** Heat index. **F:** Aridity. In each case, values are shown in gray-scale with black for lowest values and white for highest values.

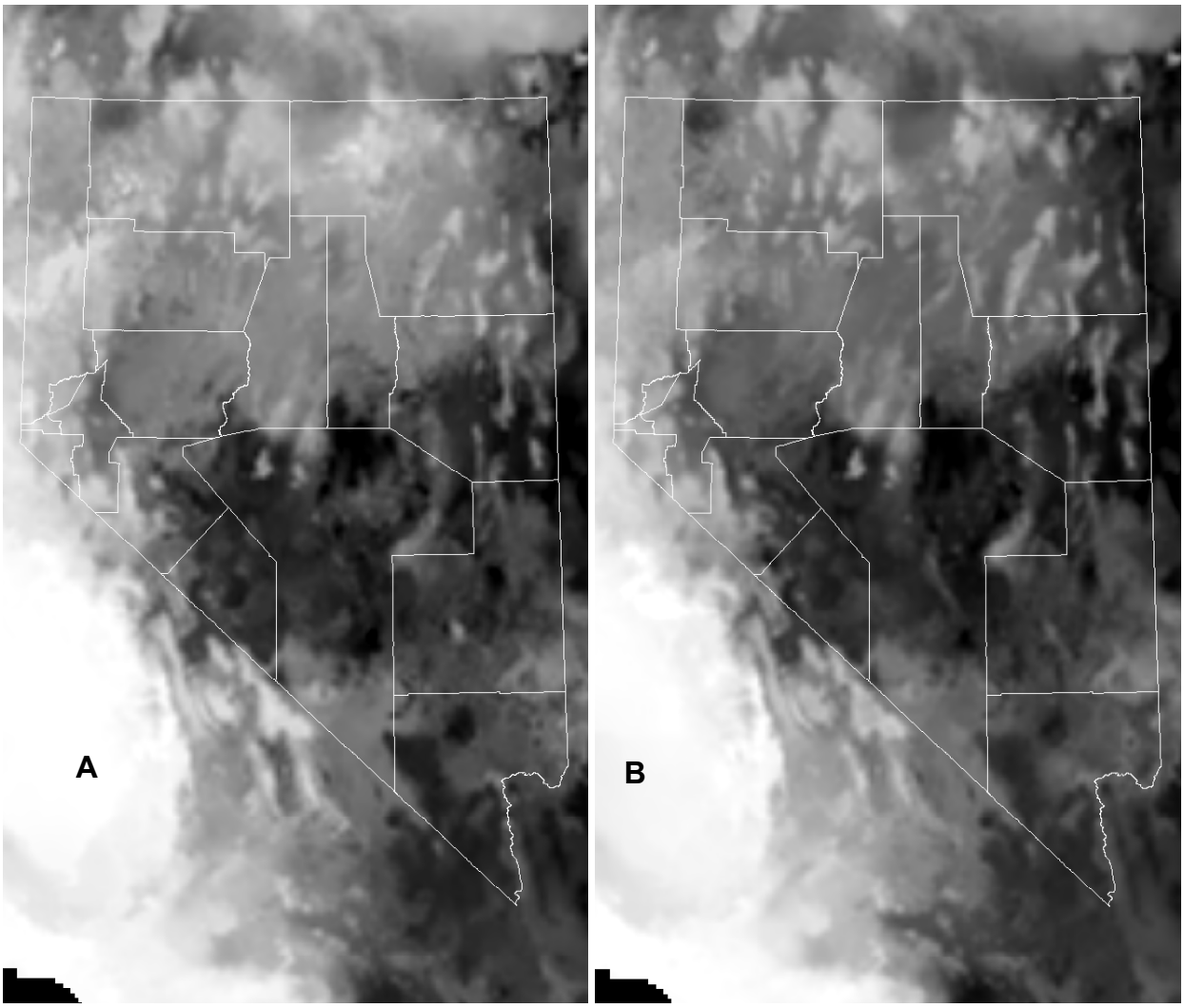

Figure 7: Seasonal variation in precipitation. **A:** Contrast of January versus August totals. **B:** Contrast of January through March versus July through September totals. Winter dominated precipitation is white while summer dominated precipitation is black. Calculations are based on PRISM precipitation models (Spatial Climate Analysis Service, Oregon State University 2003); see methods for details.

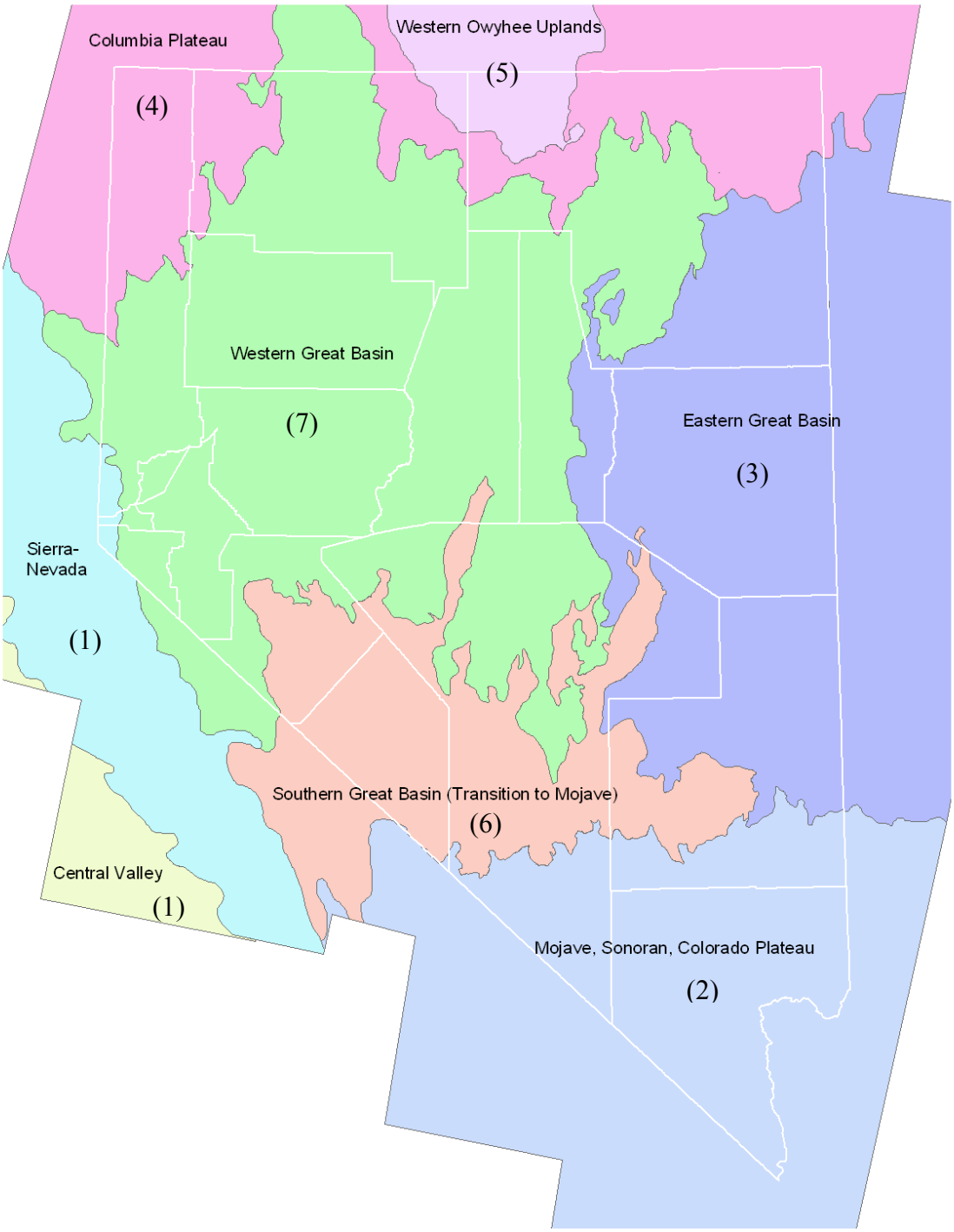

Figure 8: Annual grass focused ecoregions used in modeling. Ecoregional boundaries are based in part on region and subregion mapping by Bryce et al. (2003) but have been substantially grouped and edited based on personal field experience during training data collection. Numbers given refer to the Region*X* binary variables used in models.

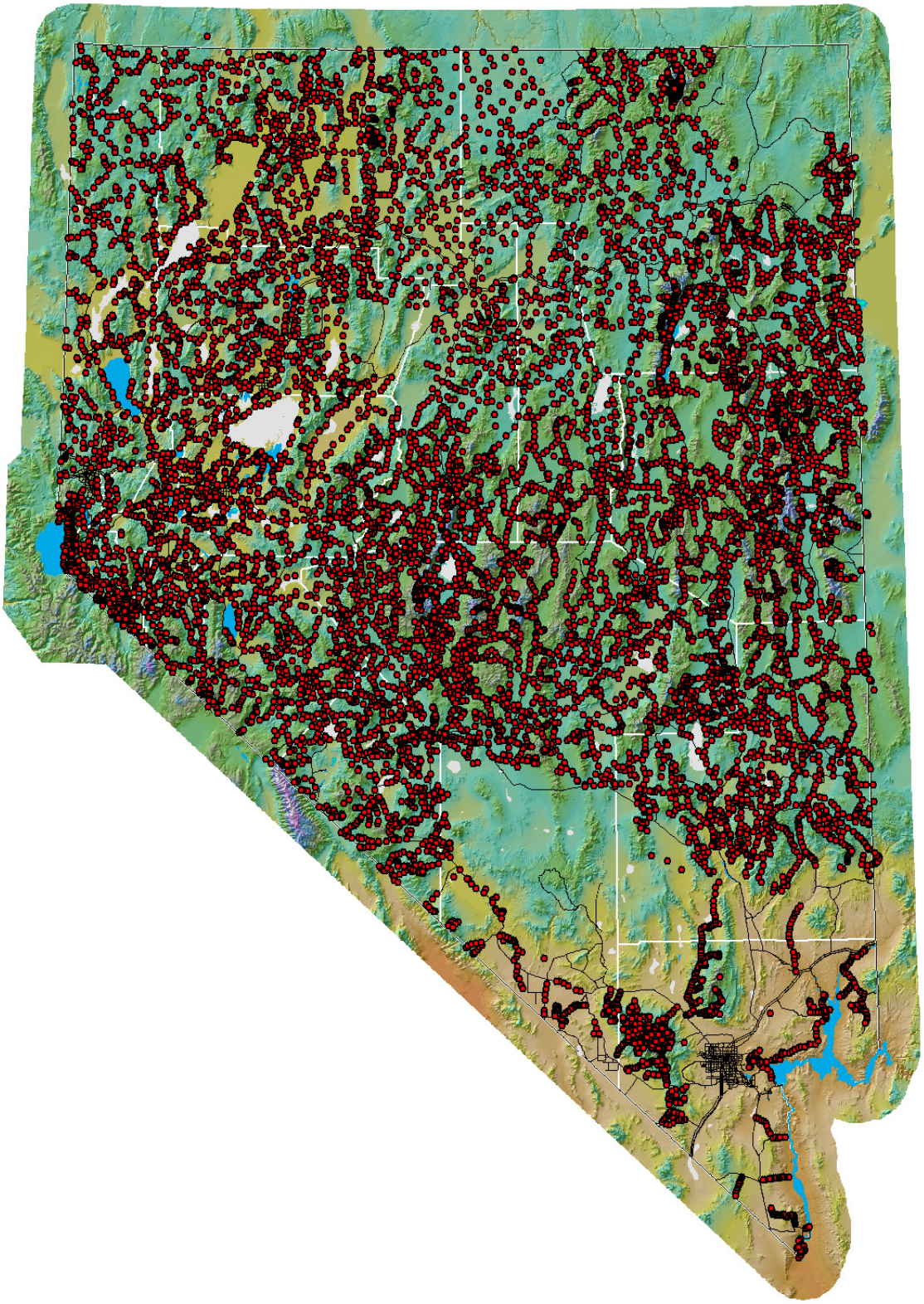

Figure 9: Plots gathered by the Southwest Regional Gap Analysis Project (Lowry et al. 2005) used herein for accuracy assessment (REGAP data set).

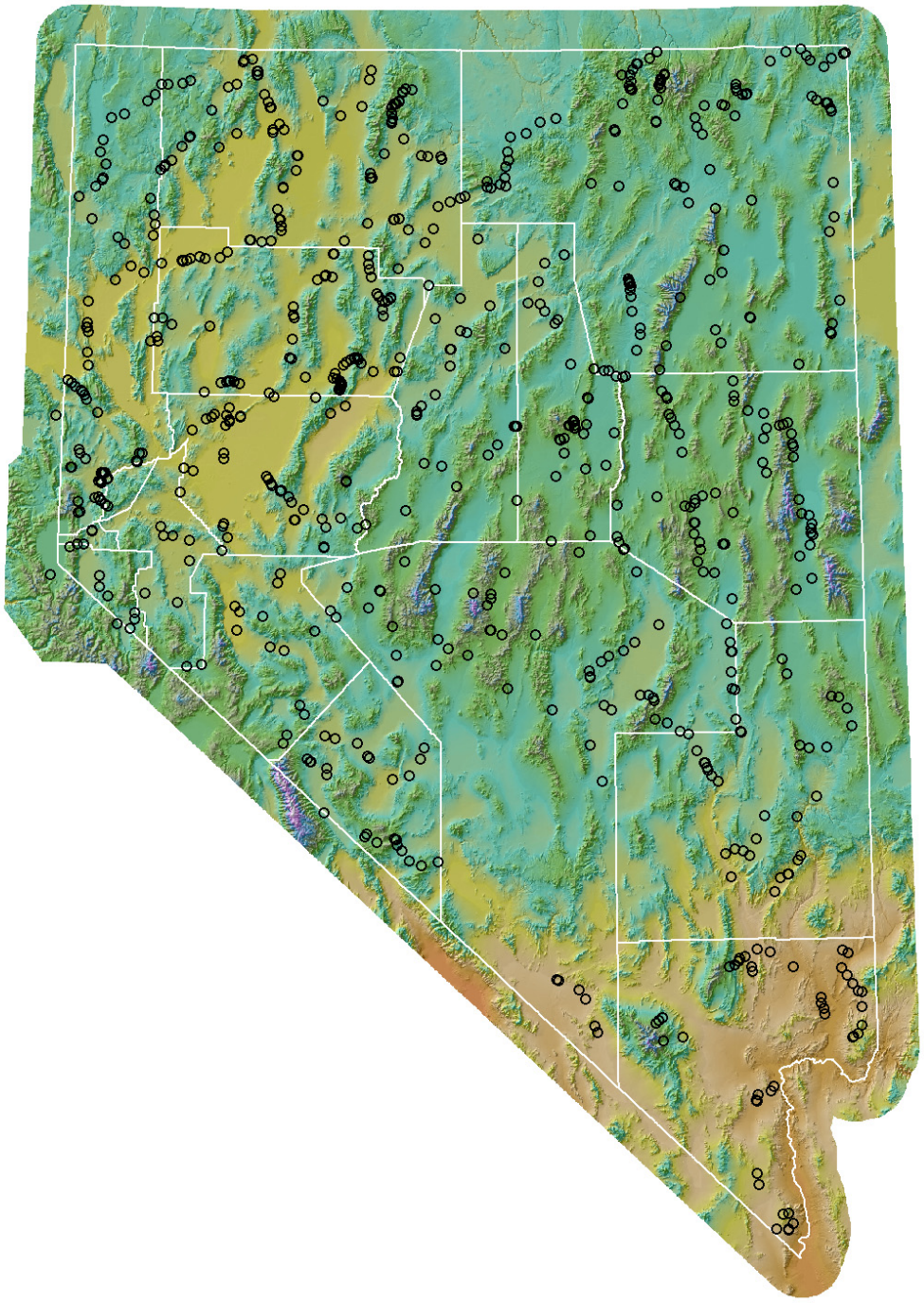

Figure 10: Geographic distribution of training data plots collected by the Nevada Natural Heritage Program, years 2002 to present.

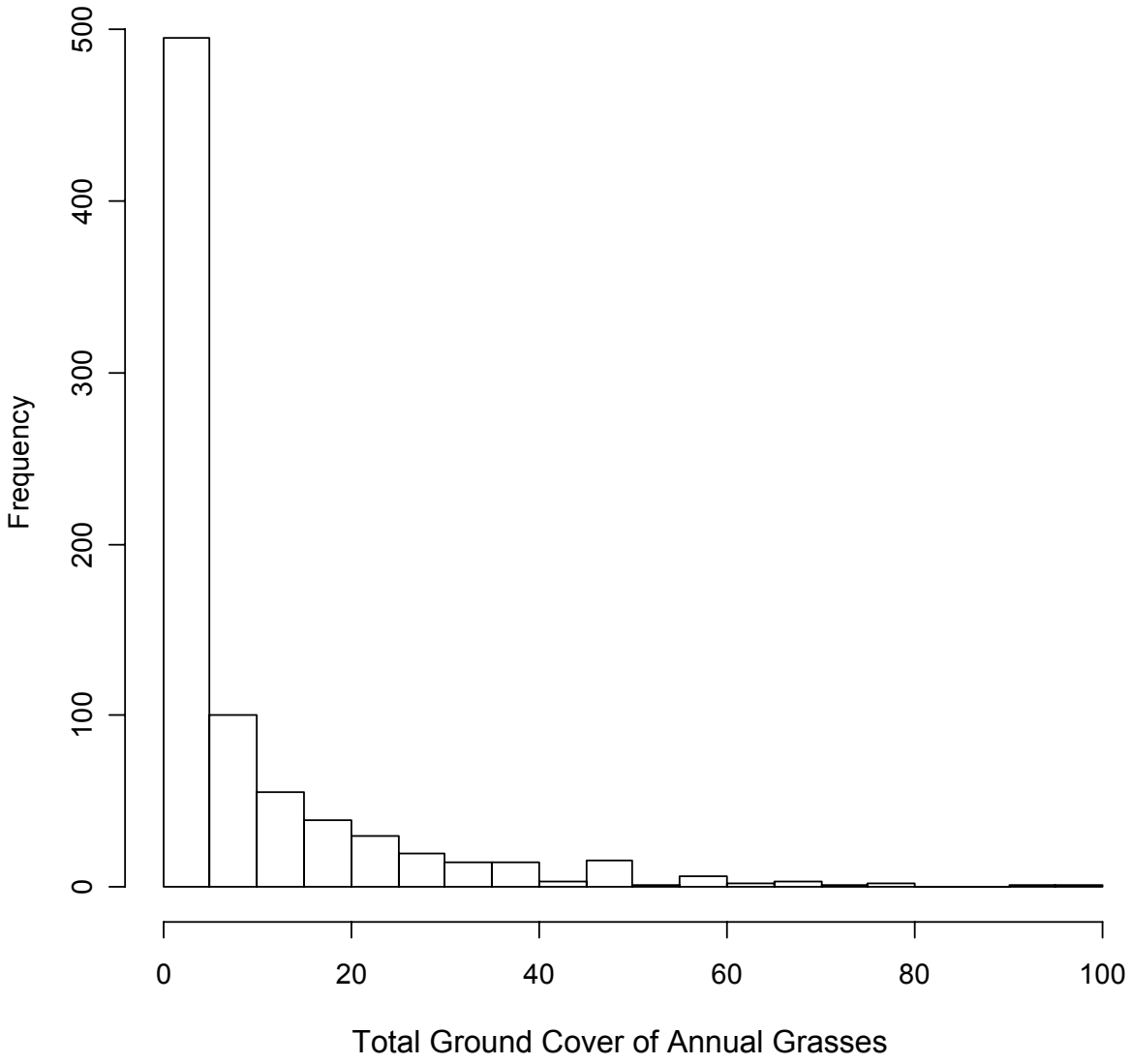

Figure 11: Histogram of percent ground-cover for annual grasses in training data plots. Each bar covers a 5 percent range.

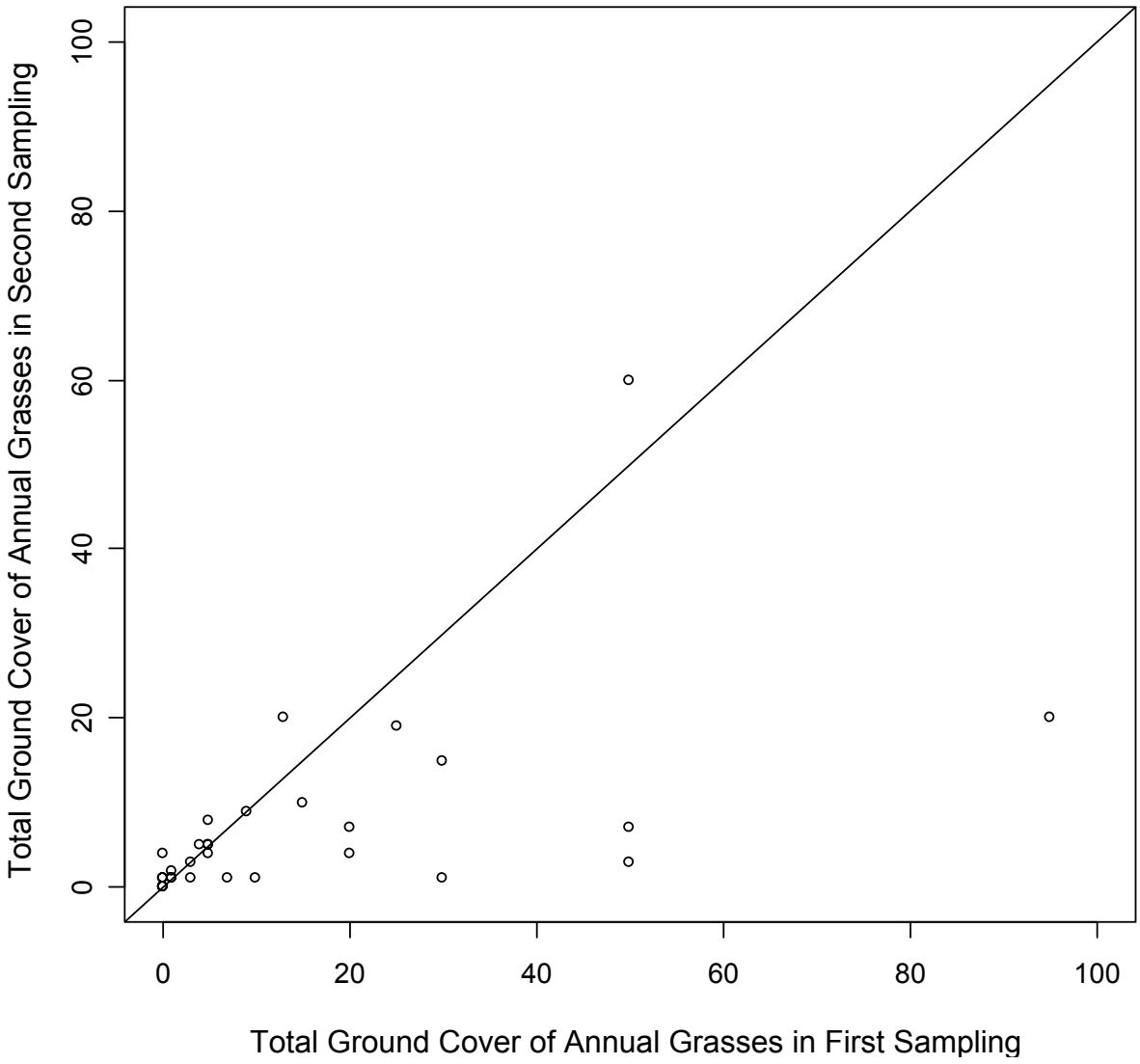

Figure 12: Scatter plot of total annual grass ground-cover at 30 repeated plots in 2002 or 2003 versus 2005 ($R = 0.54$). Plots above the diagonal line increased in measured ground-cover while plots below the line reduced in measured ground-cover. Several plots overlap at the origin.

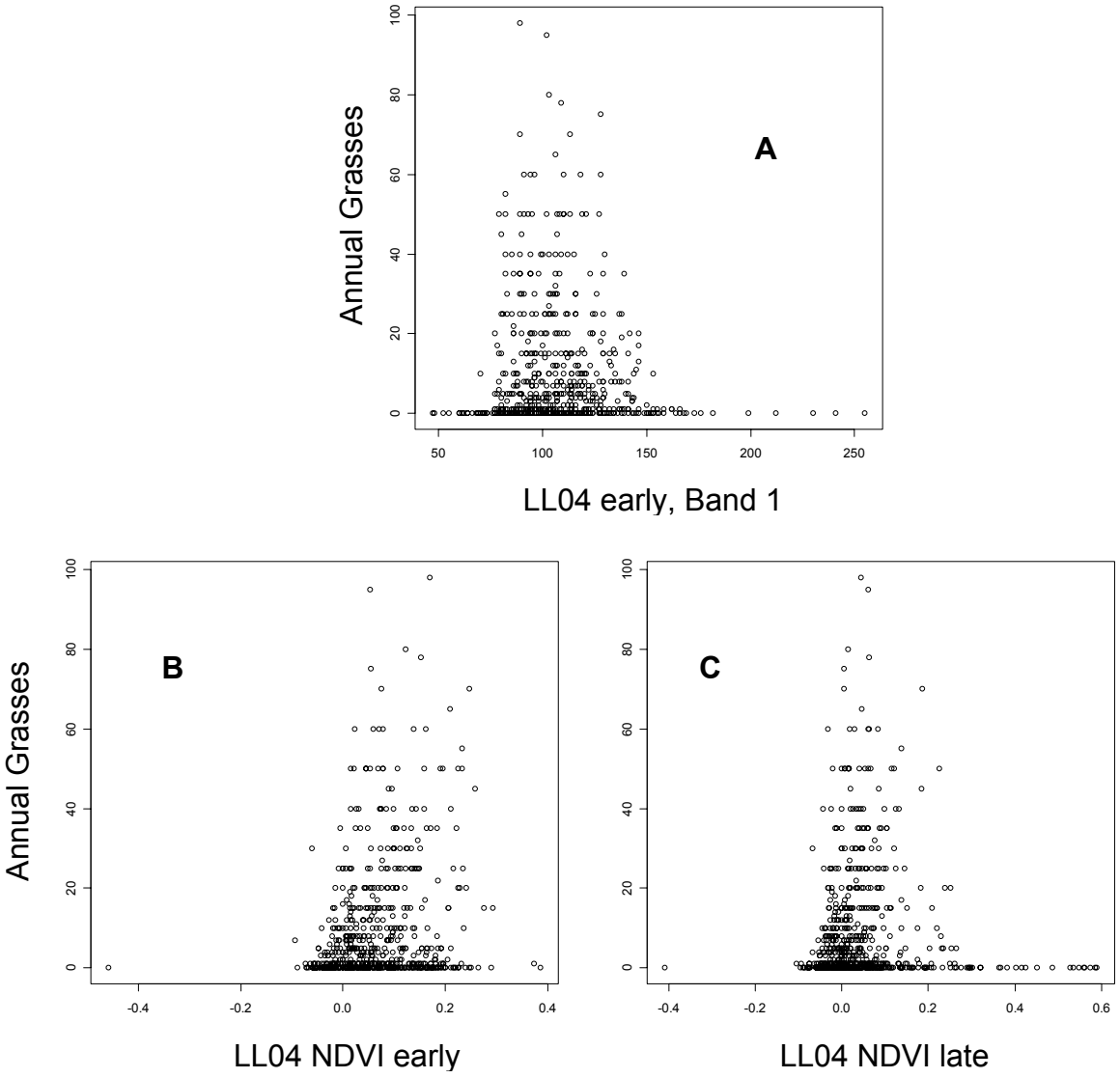

Figure13: Scatter plots showing percent ground-cover of annual grasses at training sites where un-clouded 2004 Landsat data were available. **A:** Plotted over Landsat 5 spectral band 1 (early season). **B:** Plotted over NDVI calculated from early season Landsat data. **C:** Plotted over NDVI calculated from late season Landsat data. These graphs were used in deciding cutoffs for windowing potential for annual grass index greater than zero.

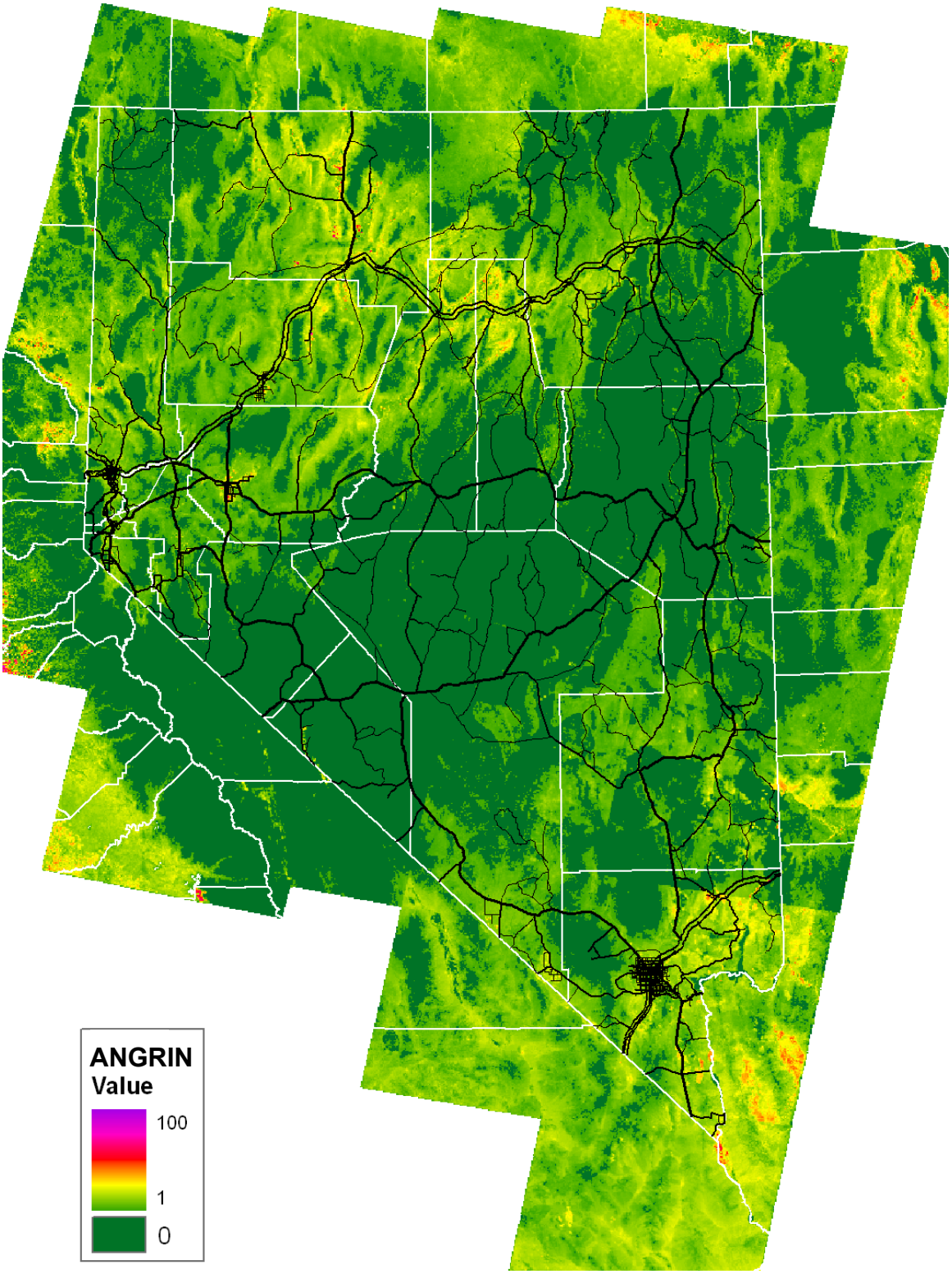

Figure 14: Annual grass index (ANGRIN), as calculated geographically over the satellite sensor data set.

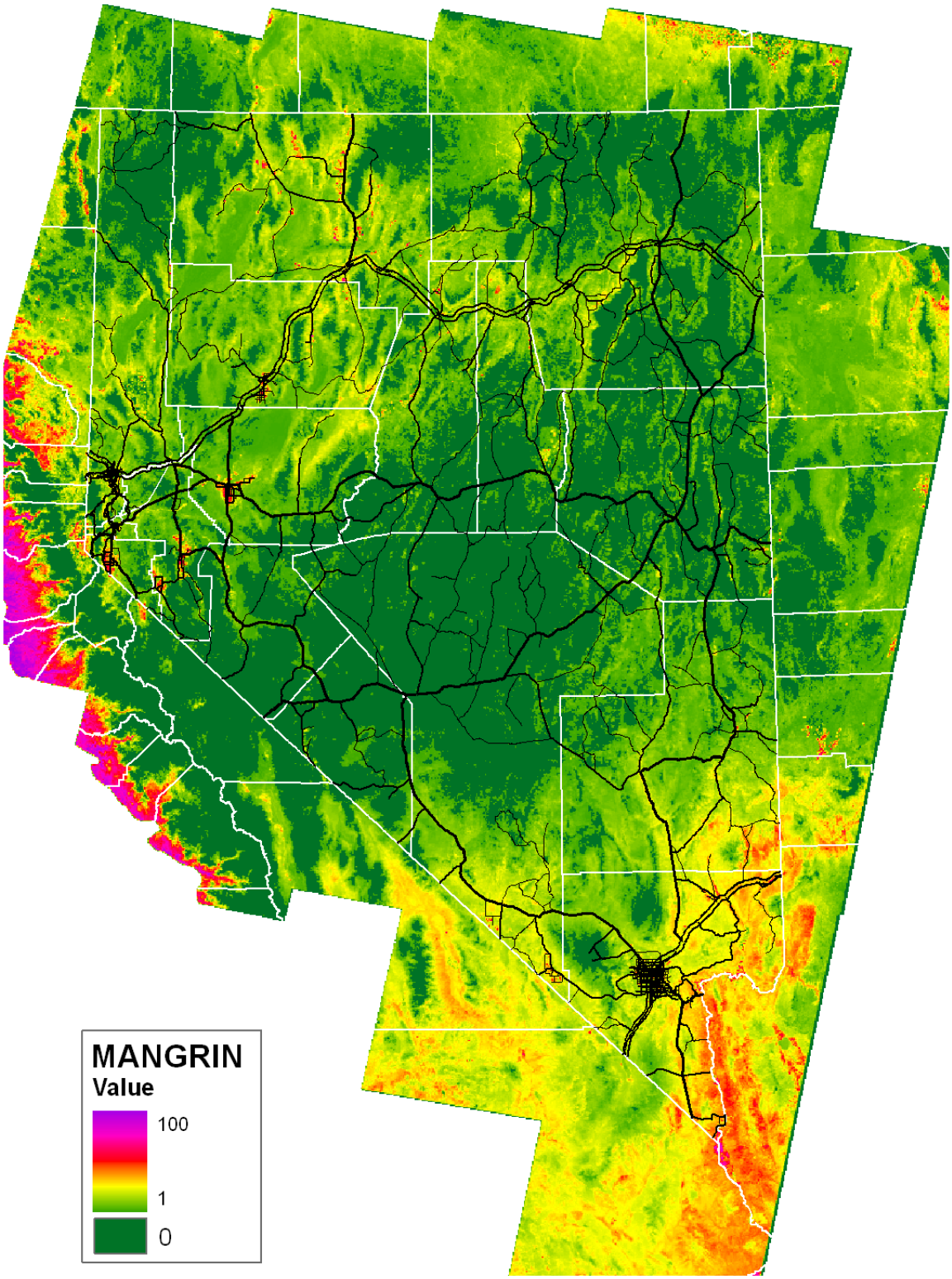

Figure 15: MODIS-only annual grass index (MANGRIN) as calculated geographically from 2004 data for the more northerly ecoregions and 2005 for the Mojave and southern Great Basin ecoregions.

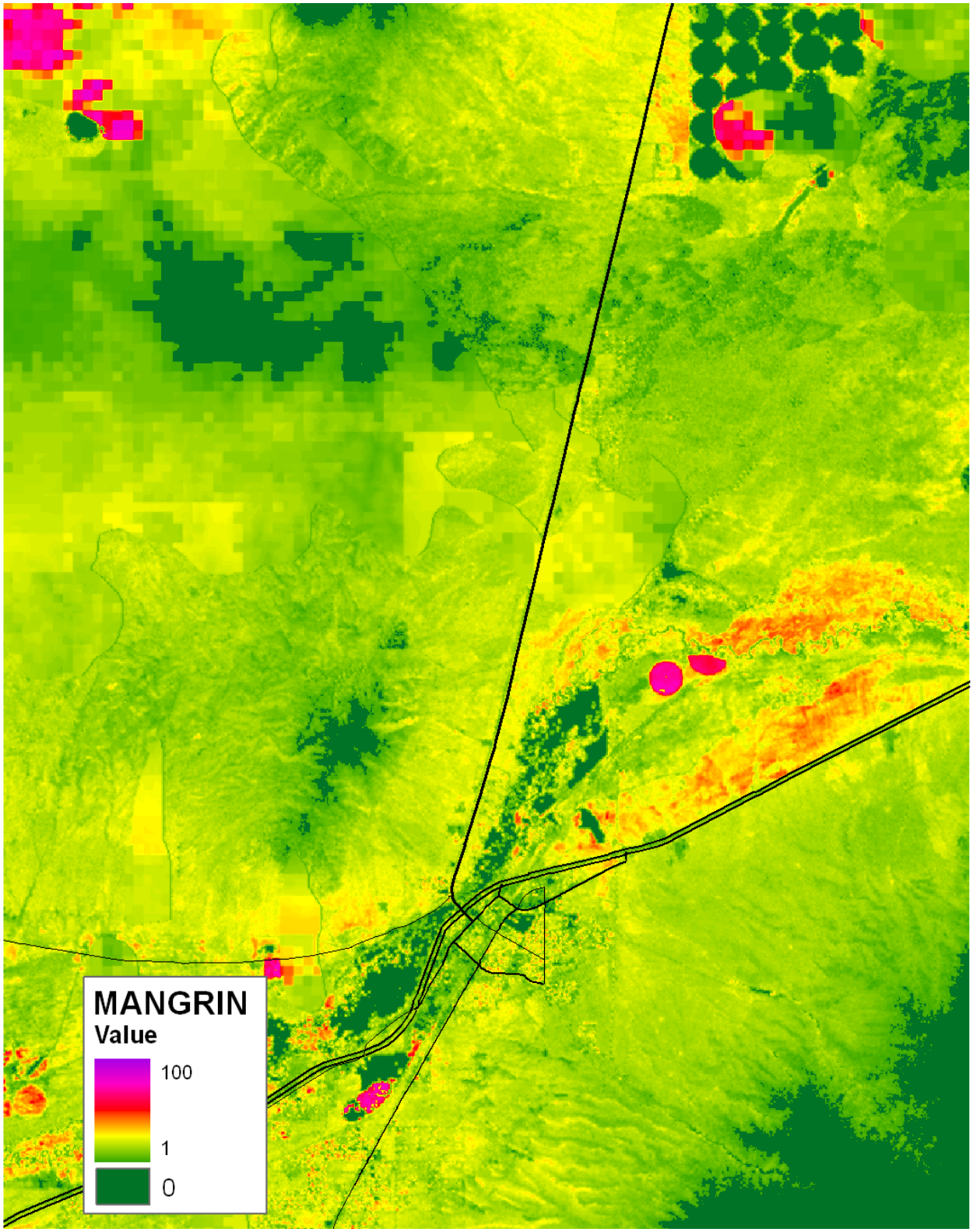

Figure 16: Final ANGRIN map showing the Winnemucca area where numerous 'cloud-holes' from the Landsat 5 data were filled with the 2004 MODIS model. Portions of the map derived from MODIS are visible through strong pixelation (blocky appearance).

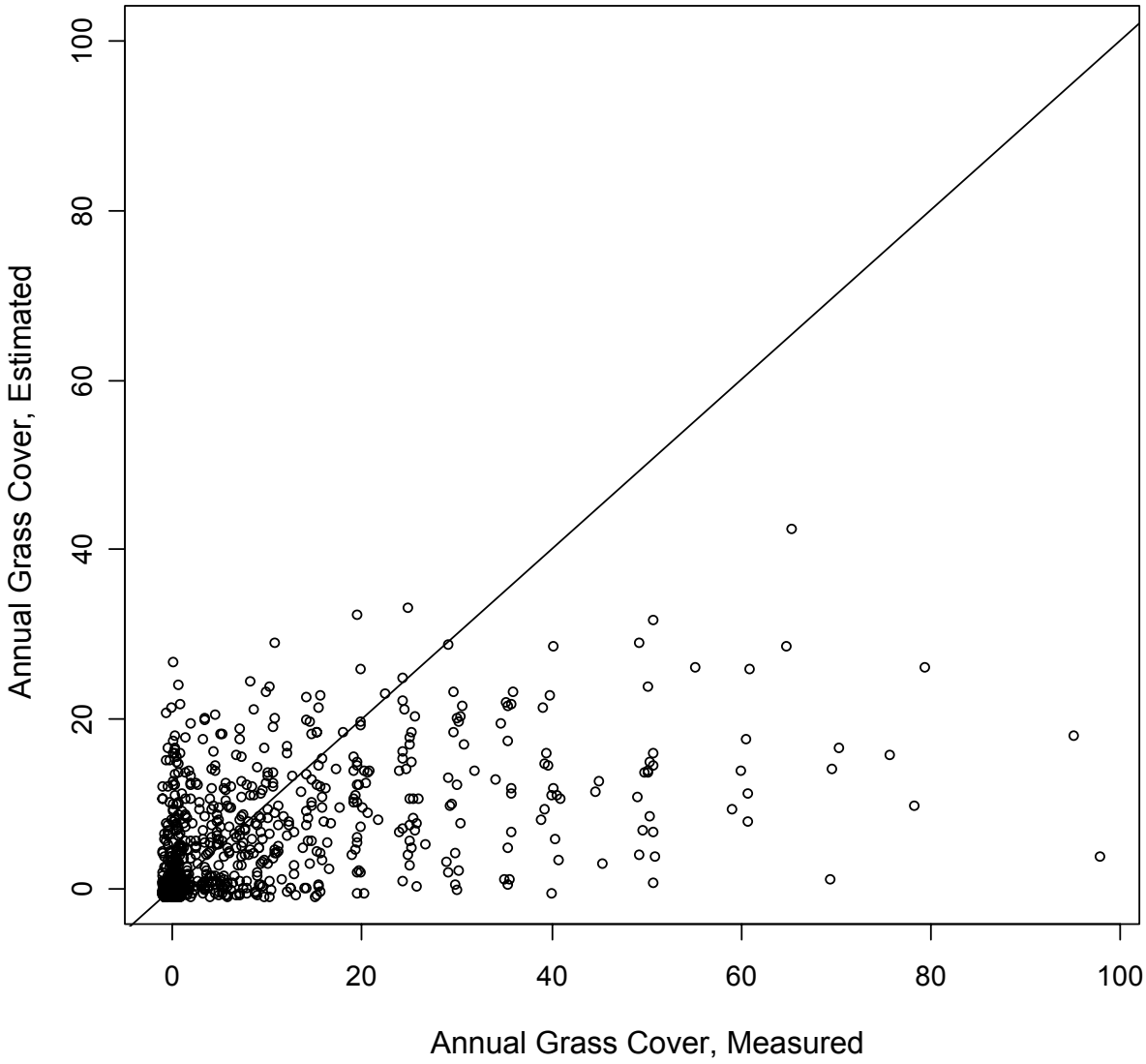

Figure 17: Correspondence between actual and predicted values for 806 training data plots (R = 0.493). The line represents the ideal 1 to 1 relationship. Use of the same data for training and for accuracy assessment commits the logical error of circularity, however this plot does demonstrate the deflated estimates at higher values, if the annual grass index (ANGRIN) is interpreted as estimated ground cover. Data are jittered to reveal overlapping points.

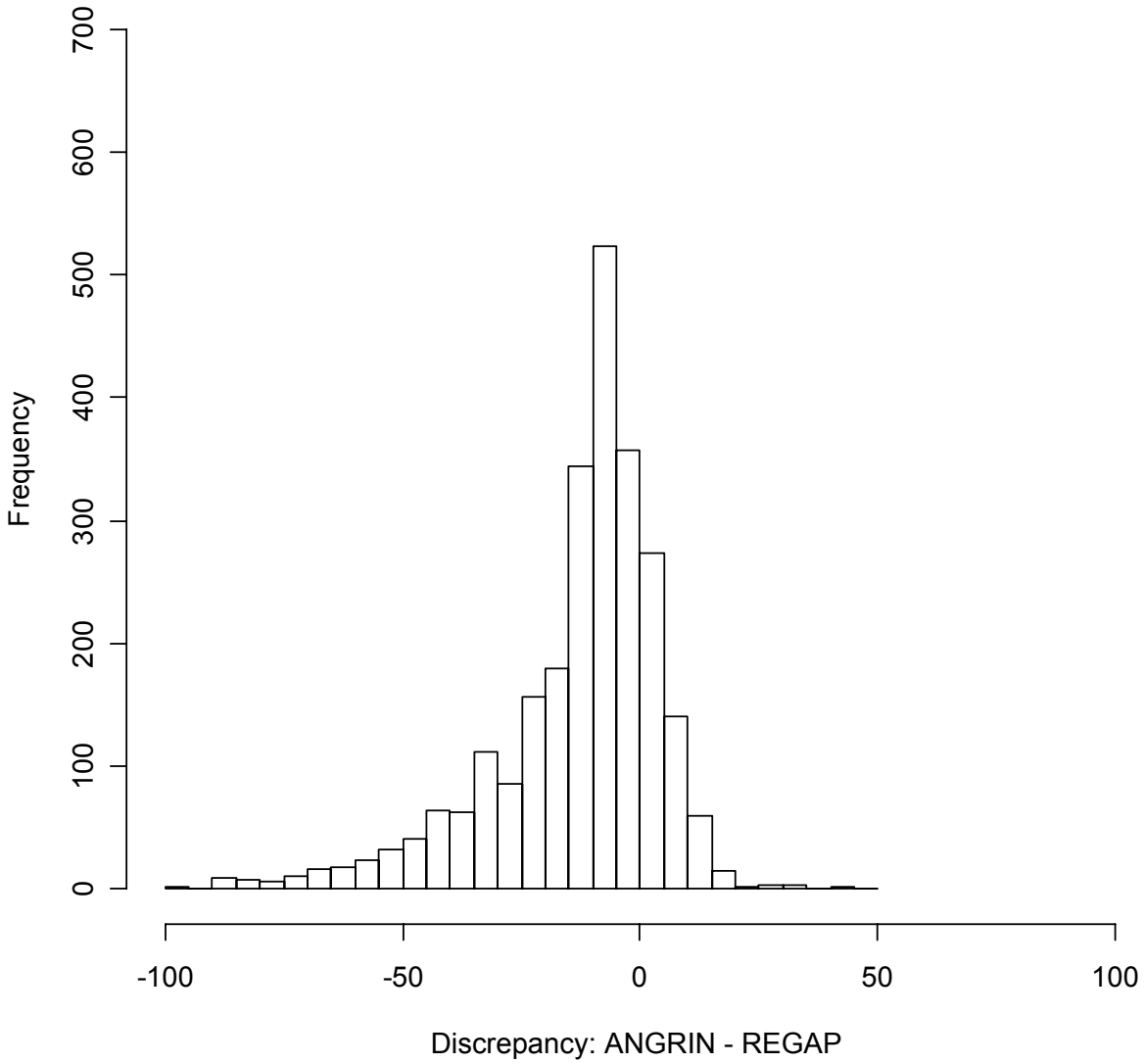

Figure 18: Histogram of discrepancy between estimated annual grass cover (ANGRIN map) and REGAP data (Lowry et al. 2005) where REGAP measured cover is greater than zero (2552 plots; these were removed to avoid such a large spike at zero that the frequency scale would render most other columns barely visible). Each bar covers a range of 5. This shows that a large portion of the plots have zero or near-zero difference. The skew toward negative difference is a result of the ANGRIN map underestimating higher values of annual grass cover.

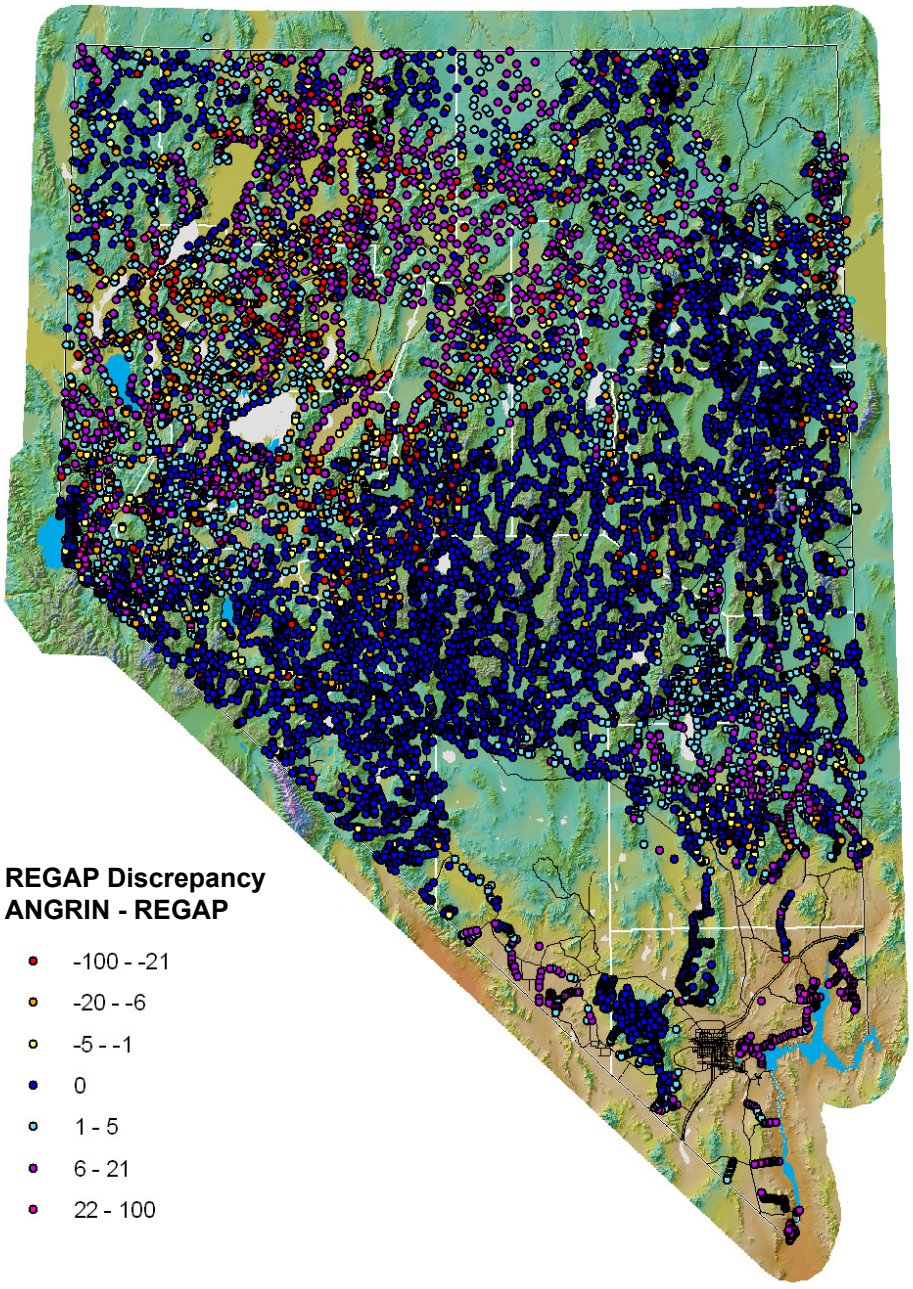

Figure 19: Geographic distribution of discrepancy between the ANGRIN map and REGAP field data.

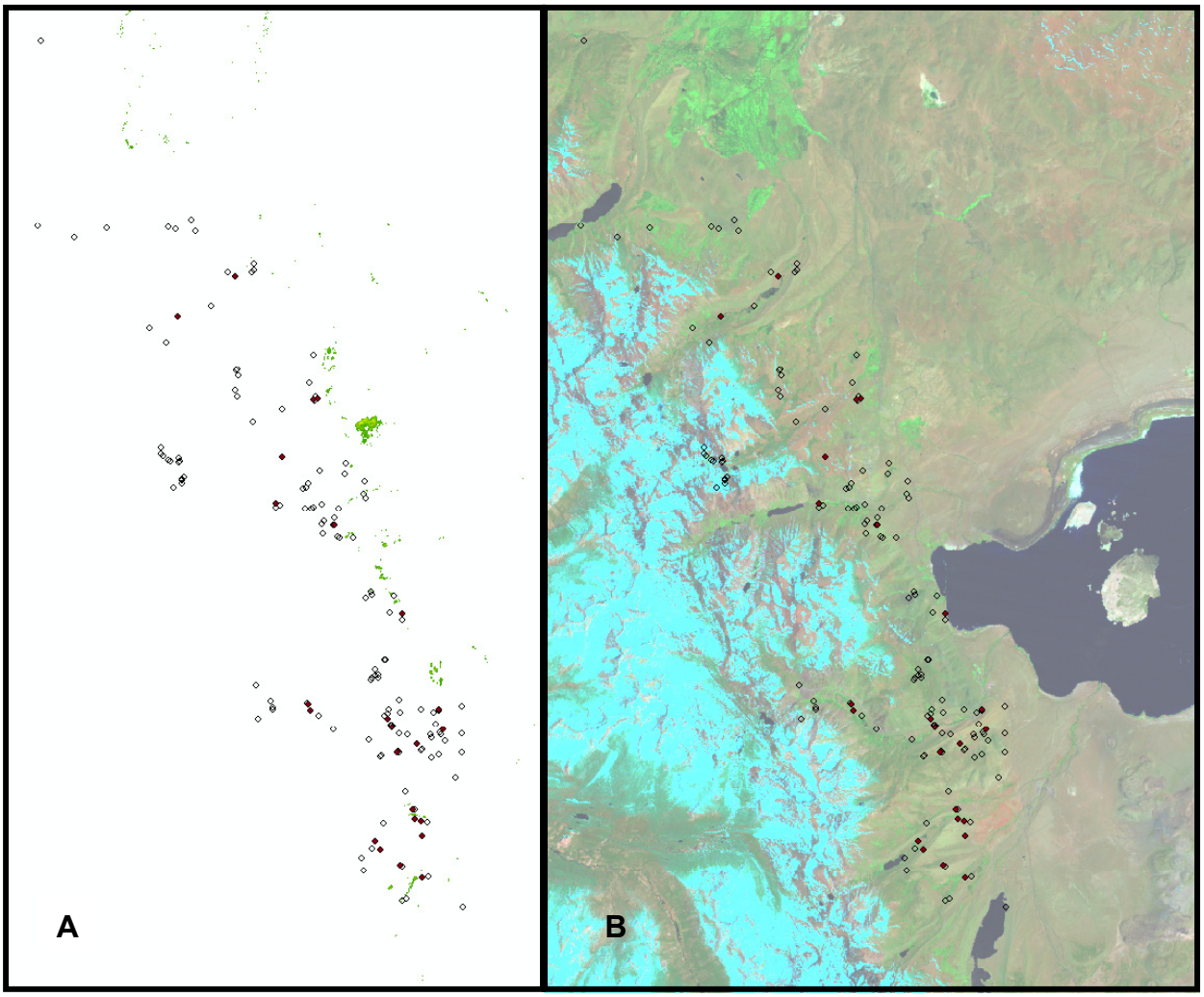

Figure 20: California Department of Fish and Game plots from Yosemite study (Keeler-Wolf et al. 2002) subset to eastern side of the Sierra-Nevada crest for comparison to the annual grass index map (178 plots – the YOSEMITE data set). **A:** Annual grass index map where greater than 0, overlaid with plots (open circles have zero cover of annual grasses, filled circles have 1 percent or more ground cover of annual grasses). **B:** Plots overlaying a false-color Landsat image to show geographic position of plots relative to Mono Lake (light blue = snow cover).

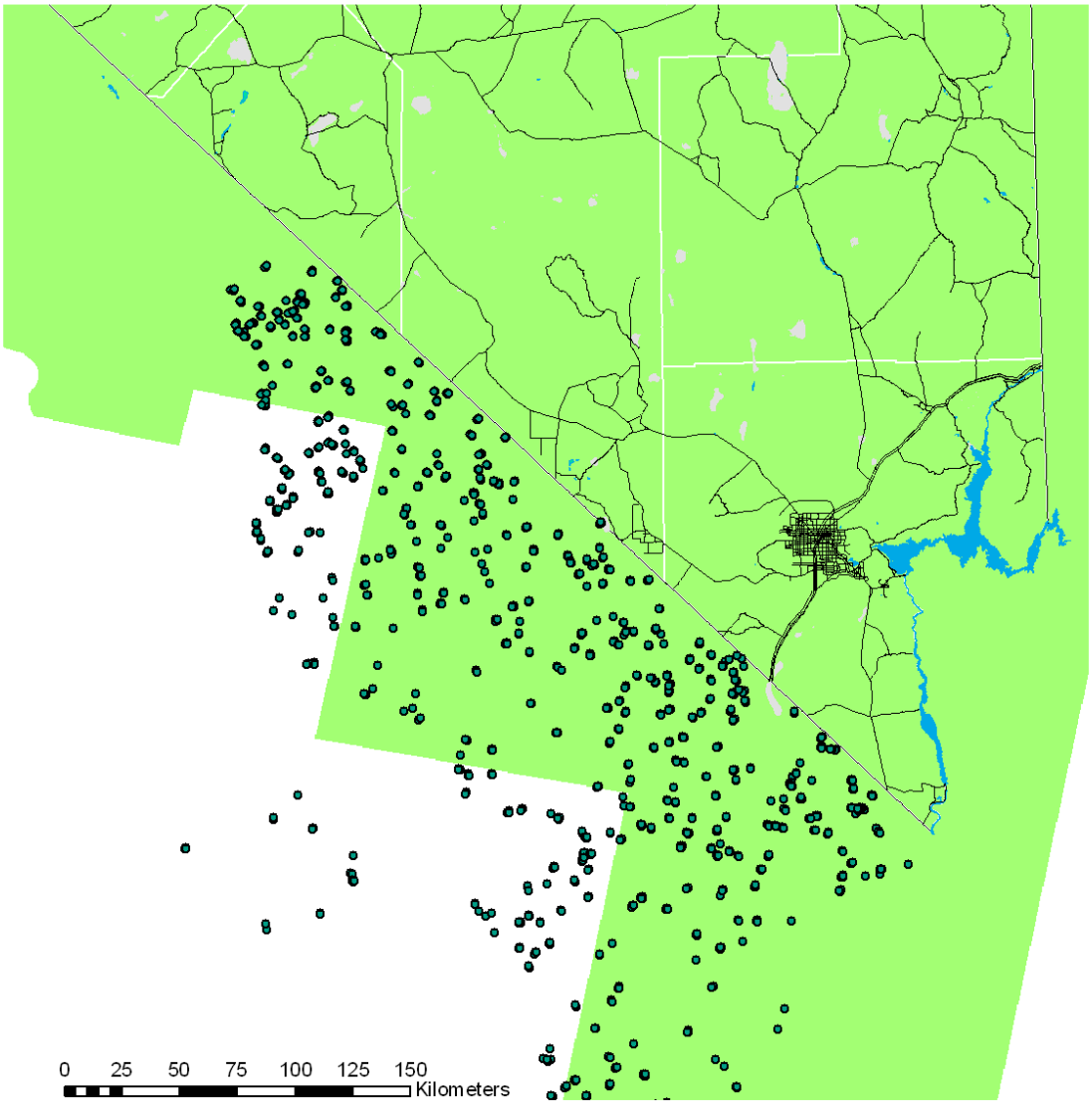

Figure 21: Distribution of California Department of Fish and Game plots in the Mojave ecoregion (Thomas et al. 2002, 2004). The green background shows the footprint of the Landsat sensor data used in this project. Plots displayed here that overly the Landsat footprint are included in the MOJAVE data set.

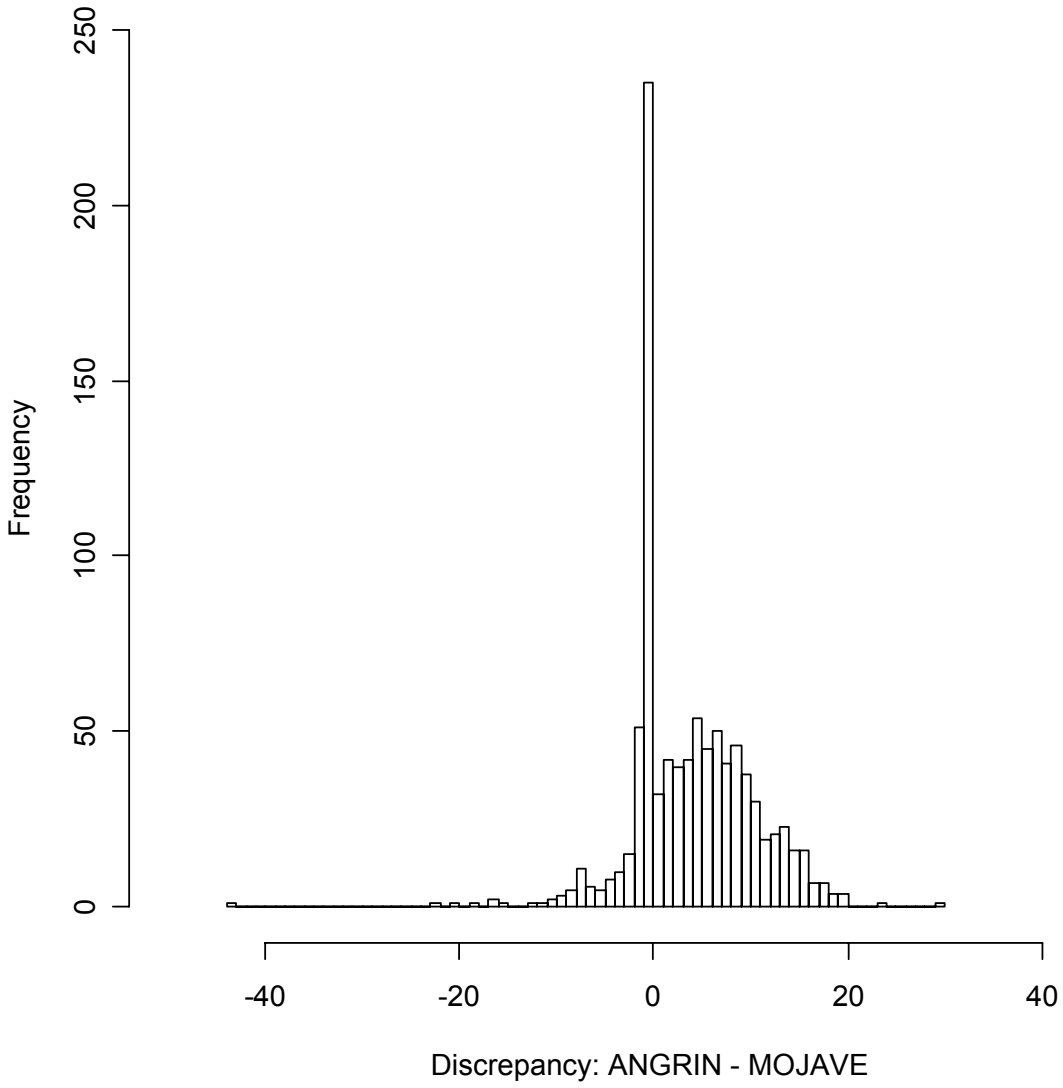

Figure 22: Histogram of discrepancy between estimated annual grass cover (ANGRIN map) and California Department of Fish and Game MOJAVE data (939 plots). Each bar covers a range of one. This shows that a large portion of the plots have zero difference, and that the majority of the plots where there is a difference, the difference is positive. This would be expected, as the ANGRIN map is derived from an exceptionally wet year while the MOJAVE data are mainly from relatively dry years. Furthermore, other early-season annual plants in the Mojave were probably also included in the ANGRIN map.